



Article

Modification of Variance-Based Sensitivity Indices for Stochastic Evaluation of Monitoring Measures

David Sanio ^{*} , Mark Alexander Ahrens and Peter Mark

Institute of Concrete Structures, Ruhr-University Bochum, 44780 Bochum, Germany; alexander.ahrens@rub.de (M.A.A.); peter.mark@rub.de (P.M.)

^{*} Correspondence: david.sanio@rub.de; Tel.: +49-(0)234-32-26065

Abstract: In complex engineering models, various uncertain parameters affect the computational results. Most of them can only be estimated or assumed quite generally. In such a context, measurements are interesting to determine the most decisive parameters accurately. While measurements can reduce parameters' variance, structural monitoring might improve general assumptions on distributions and their characteristics. The decision on variables being measured often relies on experts' practical experience. This paper introduces a method to stochastically estimate the potential benefits of measurements by modified sensitivity indices. They extend the established variance-based sensitivity indices originally suggested by Sobol'. They do not quantify the importance of a variable but the importance of its variance reduction. The numerical computation is presented and exemplified on a reference structure, a 50-year-old pre-stressed concrete bridge in Germany, where the prediction of the fatigue lifetime of the pre-stressing steel is of concern. Sensitivity evaluation yields six important parameters (e.g., shape of the $S-N$ curve, temperature loads, creep, and shrinkage). However, taking into account individual monitoring measures and suited measurements identified by the modified sensitivity indices, creep and shrinkage, temperature loads, and the residual pre-strain of the tendons turn out to be most efficient. They grant the highest gains of accuracy with respect to the lifetime prediction.

Keywords: sensitivity analysis; probability; probabilistic methods; Monte Carlo; monitoring; lifetime prediction; concrete bridge



Citation: Sanio, D.; Ahrens, M.A.; Mark, P. Modification of Variance-Based Sensitivity Indices for Stochastic Evaluation of Monitoring Measures. *Infrastructures* **2021**, *6*, 149. <https://doi.org/10.3390/infrastructures6110149>

Academic Editors: Carlo Rainieri, Andy Nguyen, You Dong and Dmitri Tcherniak

Received: 1 October 2021
Accepted: 22 October 2021
Published: 23 October 2021

Publisher's Note: MDPI stays neutral with regard to jurisdictional claims in published maps and institutional affiliations.



Copyright: © 2021 by the authors. Licensee MDPI, Basel, Switzerland. This article is an open access article distributed under the terms and conditions of the Creative Commons Attribution (CC BY) license (<https://creativecommons.org/licenses/by/4.0/>).

1. Introduction

Engineers use mathematical models to describe the bearing behavior of structures or to predict their residual lifetime [1]. Here, usually many and partially interactive parameters need to be considered [2], for instance, material properties [3], loads [4] and dimensions [5]. To account for uncertainty, they are included as variables in stochastic simulations [6–9].

Sensitivity analyses (SA) are well established to investigate and analyze analytical or numerical computational models [10,11]. They help to improve the knowledge on the model's behavior and to assess the impact of all parameters to the variability of the model output [12]. During the last decades, alternative methods have been developed and enhanced [13]. While in case of simple models, the impact of a single variable might already be identified analytically or employing local SA, more complex models—quite common in engineering—usually require more sophisticated global methods [14]. Global methods can be further divided into quantitative and qualitative approaches. For an initial screening and to identify less relevant parameters [15,16], qualitative, distribution-free methods like the Elementary Effect Method by Morris [17] should be preferred. By contrast, the variance-based sensitivity indices by Sobol' [18] involve substantial computational costs but also provide the most sophisticated information in model analysis by quantitative results [11]. They assess a parameter's direct influence, as well as its influence induced by correlation to others—referred to as parameter interaction. Finally, a combination of screening and quantitative methods is also possible [19].

To improve knowledge of specific parameters and to reduce uncertainty in lifetime predictions, structural monitoring is becoming more and more popular [20–22]. Measurement techniques are used to monitor the structural response [23–25] or to estimate acting loads [26]. Furthermore, material testing is commonly used to increase the accuracy [27,28]. Each measurement technique has an associated accuracy and thus a specific reduction potential of epistemic uncertainty. However, even at the highest accuracy, all parameters have a minimum natural uncertainty that cannot be further reduced (aleatory uncertainty) [29].

So far, monitoring components, sensors and parameters are usually selected by experts or according to general guidelines [30,31]. The measured variables are selected based on experience [32] or the results of structural computation. This paper presents an approach to answer the question of which parameters should be measured to achieve the highest benefit in structural computation, based on highest accuracies achievable by measurements. Therefore, not the most important parameter in the model should be identified, but that one which brings the greatest benefit if its uncertainty is reduced as much as possible.

In this paper a modification of the variance-based sensitivity indices is proposed. Based on the reduction of the epistemic uncertainty of a parameter, they can evaluate and quantify the benefit of measurements and monitoring. The method is based on the variance-based sensitivity indices by Sobol' [18], which are presented in Section 2, and the conditional variance [33,34], where a single parameter is fixed to a constant value. The modified approach is presented in Section 3 and exemplified on a practical model in Section 4. The presented model was developed to predict the residual fatigue lifetime of a pre-stressed concrete bridge.

2. Variance-Based Sensitivity Indices

Variance-based SA go back to the pioneering work of Cukier et al. [35], who considered the conditional variance as a measure of a model's sensitivity. Later, Hora and Iman [34] analyzed the variance of a model in cases when one parameter is fixed to a certain value. Finally, Sobol' derived a numerical, Monte-Carlo-based estimation of sensitivity indices [18], which covers both a parameter's direct influence as well as its interaction to others by means of the covariance [13]. In this section, the theoretical background of this SA method is given. In Section 2.2, a method of computation is briefly introduced which is later adapted to derive modified indices in Section 3.

2.1. Variance-Based Sensitivity Indices by Sobol'

A computational model describes a specific output Y based on one or a different input parameters (variables) X_i , cf. Equation (1). The uncertainty of each variable $V(X_i)$ propagates through the model and results in uncertain model output $V(Y)$. Variance-based SA determine the contribution of each parameter's uncertainty to the uncertainty of the output. For complex models, in addition to the direct variance of each parameter $V(X_i)$, covariances $V(X_i, X_j)$ and higher order variances $V(X_i, \dots, X_n)$ arise and can be relevant. Then, more sophisticated SA methods serve to identify each parameter's impact.

In general, all these methods base on variance decomposition of a model Y Equation (1) as a square-integrable function of q variables X_1, X_2, \dots, X_q in a q -dimensional unit hyper-space Ω_q ($0 \leq X_i \leq 1$).

$$Y = f(\mathbf{x}) = f(X_1, X_2, \dots, X_q) \tag{1}$$

Decomposition of Y —by means of ANOVA HDMR (analysis of variance, high dimensional model representation [36])—delivers a single constant term f_0 , q linear terms $f_i(X_i)$, q over 2 s-order terms f_{ij} and higher-order terms. Overall, the model consists of 2^q terms; each square-integrable again.

$$Y = f(\mathbf{x}) = f_0 + \sum_{i=1}^q f_i(X_i) + \sum_{i=1}^q \sum_{j>i}^q [f_{ij}(X_i, X_j) + \dots + f_{1,2,\dots,q}(X_1, X_2, \dots, X_q)] \tag{2}$$

The decomposition is not unique, but assuming all mean values except f_0 to be zero, Sobol' proved all terms being orthogonal [18]. Thus, the zero-order term f_0 corresponds to the model's expectation $E(Y)$:

$$f_0 = E(Y) \tag{3}$$

Higher-order terms can be determined by the conditional expectation $E(Y | X_i)$ (see [37]), where dx_{-i} denotes an integration over all dimensions except i ; equivalently, dx_{-ij} indicates an integration over all dimensions except i and j .

$$f_i(X_i) = E(Y | X_i) - E(Y) = \int_0^1 \dots \int_0^1 f(x) dx_{-i} - f_0 \tag{4}$$

$$f_{ij}(X_i, X_j) = E(Y | X_i, X_j) - f_i - f_j - E(Y) = \int_0^1 \dots \int_0^1 f(x) dx_{-\{i,j\}} - f_i(X_i) - f_j(X_j) - f_0 \tag{5}$$

In this way, the model's variance $V(Y) = E(Y^2) - E(Y)^2 = \int_{\Omega_q} f^2(x) dx - f_0^2$ can be decomposed in first- and higher-order terms, respectively (Equation (6)). Here, the second-order variance V_{ij} of two parameters X_i and X_j is the covariance and is a measure of interaction.

$$V(Y) = \sum_{i=1}^q V_i + \sum_{i=1}^q \sum_{j>i}^q [V_{ij} + \dots + V_{1,2,\dots,q}] \tag{6}$$

From this, the first order sensitivity index S_i follows as the ratio of the model's conditional variance $V(E(Y | X_i))$, when all parameters but X_i are fixed, to the variance of the entire model $V(Y)$ with all parameters variable.

$$S_i = \frac{V(f_i(X_i))}{V(Y)} = \frac{V(E(Y | X_i))}{V(Y)} \tag{7}$$

Thus, single S_i -values quantify the direct impact of an individual variance on the model result Y . Higher-order sensitivity indices ($S_{ij}, \dots, S_{1,2,\dots,q}$) can be deduced from conditional variances as well (see [10]). Those are measures of interaction of two (covariance) or more parameters (higher-order variance). Restricting on a single parameter X_i for convenience, its total sensitivity index S_{Ti} represents the ratio of its direct influence on the model's variance V_i (conditional variance) and all covariances of X_i (V_{ij}, V_{ijk}, \dots) in relation to the model's variance. To prevent the conditional variance from being dependent on a fixed value $X_i = x_i^*$, the expectation of the conditional variance $V_{x-i}(X_i = x_i^*)$ over the range of x_i^* denoted $E_{X_i}(V_{x-i}(X_i = x_i^*)) = E(V(Y | X_i))$ is calculated [10].

$$\begin{aligned} V(Y) &= V(E(Y | X_i)) + E(V(Y | X_i)) \\ &= V(E(Y | X_{-i})) + E(V(Y | X_{-i})) \end{aligned} \tag{8}$$

Finally, the total sensitivity index S_{Ti} for the parameter X_i follows as the ratio of the parameter's direct variance V_i and all higher-order variances (V_{ij}, V_{ijk}, \dots) involving X_i to the variance of the entire model $V(Y)$. Thus, it quantifies the impact of all interactions involving X_i and their direct influences:

$$\begin{aligned} S_{Ti} &= 1 - \frac{V(E(Y | X_{-i}))}{V(Y)} \\ &= \frac{V_i + \sum_{j \neq i} V_{ij} + \sum_{j \neq i, k \neq j} V_{ijk} + \dots + V_{1,2,\dots,q}}{V(Y)} \\ &= S_i + \sum_{j \neq i} S_{ij} + \sum_{j \neq i, k \neq j} S_{ijk} + \dots + S_{1,2,\dots,q} \end{aligned} \tag{9}$$

In case of no interactions, all higher-order variances are zero and $S_{Ti} = S_i$.

2.2. Computation of Variance-Based Sensitivity Indices

Sensitivity indices are usually computed using Monte Carlo simulations [38]. Initially, Sobol' [18] developed an algorithm which was later enhanced by Saltelli et al. [13]. Another

modification by Glen and Isaacs [39] significantly lowers computational costs reducing the number of model simulations n necessary from n^2 to $n(2 + q)$ by calculating the correlation properties of the results. Remember that q denotes the number of parameters in the model, while the user’s choice of n comes along with the accuracy of the resulting indices and depends on the convergence of results (see Section 4.4 and [10,14,39,40]).

For computation, two independent sample matrices A and B are generated, each containing n realizations of q variables. For reliable results, the stochastic independence of A and B is essential [41]. It can be found through Pearson’s coefficient of correlation $\rho_{A,B} \approx 0$. Otherwise, even small correlations can be found as spurious correlations in the resulting sensitivity indices [39]. Especially for models with several parameters, the sensitivity indices are likely to be close to zero. Here, spurious correlations can distort the results.

$$A = \begin{bmatrix} x_1^{(1)} & \dots & x_i^{(1)} & \dots & x_q^{(1)} \\ \vdots & \dots & \vdots & \dots & \vdots \\ x_1^{(n)} & \dots & x_i^{(n)} & \dots & x_q^{(n)} \end{bmatrix}; B = \begin{bmatrix} x_{q+1}^{(1)} & \dots & x_{q+i}^{(1)} & \dots & x_{2q}^{(1)} \\ \vdots & \dots & \vdots & \dots & \vdots \\ x_{q+1}^{(n)} & \dots & x_{q+i}^{(n)} & \dots & x_{2q}^{(n)} \end{bmatrix} \tag{10}$$

In a second step, q further matrices C_i (with $i = 1, \dots, q$) are assembled from A and B . They are generated by interchanging columns. This means that the new matrix C_i is identical to B , solely column i (for parameter i) is taken from matrix A instead. Other matrices C_i are obtained analogously.

$$C_i = \begin{bmatrix} x_{q+1}^{(1)} & \dots & x_{q+i-1}^{(1)} & x_i^{(1)} & x_{q+i+1}^{(1)} & \dots & x_{2q}^{(1)} \\ \vdots & \dots & \vdots & \vdots & \vdots & \dots & \vdots \\ x_{q+1}^{(n)} & \dots & x_{q+i-1}^{(n)} & x_i^{(n)} & x_{q+i+1}^{(n)} & \dots & x_{2q}^{(n)} \end{bmatrix} \tag{11}$$

By model computation the result vectors $\mathbf{a} = Y(A)$, $\mathbf{b} = Y(B)$ and $\mathbf{c}_1 = Y(C_1)$ to $\mathbf{c}_q = Y(C_q)$ are determined. Finally, the sensitivity indices are obtained based on correlation properties between c_i and \mathbf{a} or c_i and \mathbf{b} , respectively. For details see [39].

3. Method: Modification of Variance-Based Sensitivity Indices

By means of sensitivity indices, the influence of a single parameter on the entire model can be analyzed based on its variance. Hora and Iman [34] introduced the conditional variance of a model, when one of its parameters is fixed to a deterministic value. In fact, the individual variances in stochastic analyses usually contain aleatory (random, nonreducible) and epistemic (reducible, inaccurate knowledge) parts. For structural systems only epistemic variances can be reduced (Figure 1). To determine the benefits of increased knowledge by monitoring or other measurements to reduce the variance, modified sensitivity indices should consider individual variance reductions, not the variance itself.

3.1. Proposed Method Based on SOBOL’ Indices

The proposed method decomposes the variance of a general model Y —no matter if analytical or numerical. While the initial model with originally large variances of all variables is termed Y_0 (cf. Equation (1)), the best model with utmost reduced variances is denoted Y^* . It comprises q parameters X_i^* , each having a reduced variance V^* (represented by a reduced standard deviation σ^* in Figure 1).

$$Y^* = f\left(X_1^*, \dots, X_i^*, \dots, X_q^*\right) \tag{12}$$

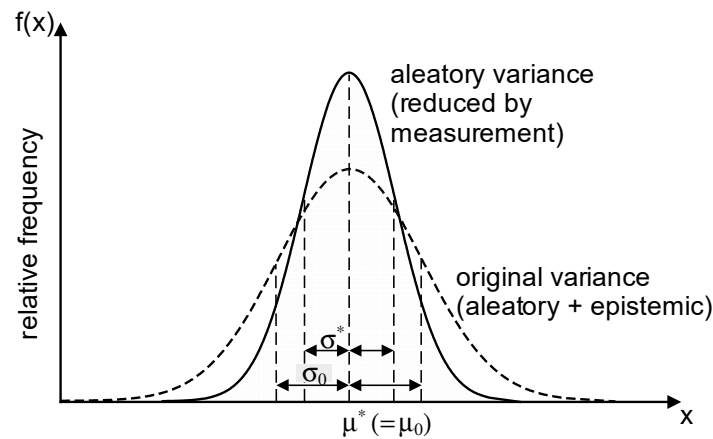


Figure 1. Probability density functions of a variable with original and reduced variance due to increased knowledge.

Both models can be reformulated mathematically by means of variance decomposition (ANOVA HDMR), as shown before.

$$V(Y_0) = \sum_{i=1}^q V_{i,0} + \sum_{i=1}^q \sum_{j>i}^q [V_{i,j,0} + \dots + V_{1,2\dots q,0}] \tag{13}$$

$$V(Y^*) = \sum_{i=1}^q V_i^* + \sum_{i=1}^q \sum_{j>i}^q [V_{i,j}^* + \dots + V_{1,2\dots q}^*] \tag{14}$$

Thus, the variance $V(Y_0)$ of the initial model Y_0 consists of q first-order variances $V_{i,0}$ and $(q \text{ over } 2)$ covariance terms $V_{i,j,0}$ (cf. Equation (6)). Y^* is treated equivalently. Thus, the difference of the two decomposed variances in Equations (15) and (16) captures the extent of potential variance reduction ΔV^* .

$$\Delta V^* = V(Y_0) - V(Y^*) \tag{15}$$

Employing Equations (15) and (16), this reduced variance can be decomposed, too. This decomposition is just analogous to that one in Section 2.2.

$$\Delta V^* = \sum_{i=1}^q V_{i,0} + \sum_{i=1}^q \sum_{j>i}^q [V_{i,j,0} + \dots + V_{1,2\dots q,0}] - \sum_{i=1}^q V_i^* - \sum_{i=1}^q \sum_{j>i}^q [V_{i,j}^* + \dots + V_{1,2\dots q}^*] \tag{16}$$

Herein, the reduced variance V_i^* of a single parameter is interpreted as its individual improvement and it reads:

$$\Delta V_i = V_{i,0} - V_i^* \tag{17}$$

Thus, the potential variance reduction ΔV^* from Equation (16) is given by:

$$\Delta V^* = \sum_{i=1}^q \Delta V_i + \sum_{i=1}^q \sum_{j>i}^q [\Delta V_{i,j} + \dots + \Delta V_{1,2\dots q}] \tag{18}$$

If at first only a single parameter X_i^* out of the q variables is improved, the model can be written as a function of $q-1$ "original" parameters $X_{j \neq i,0}$ and one "improved" parameter X_i^* .

$$Y = f(X_{1,0}, \dots, X_{i-1,0}, X_i^*, X_{i+1,0}, \dots, X_{q,0}) = Y(X_{j \neq i,0}, X_i^*) \tag{19}$$

Denoting the variance of this partly improved model $V(Y(X_{j \neq i,0}, X_i^*))$, the variance reduction by an improved knowledge about one parameter's variance follows:

$$\Delta V_i^* = V(Y_0) - V(Y(X_{j \neq i,0}, X_i^*)) \tag{20}$$

Now, considering two "improved" parameters X_i^* and X_j^* , the variance reduction of the entire model follows:

$$\Delta V_{i,j}^* = V(Y_0) - V\left(Y\left(X_{k \neq i,k \neq j,0}, X_i^*, X_j^*\right)\right) \tag{21}$$

In the same way, one can increase the number of parameters with reduced variance gradually until finally all parameters X_j^* except one single variable $X_{i,0}$ exhibit a reduced variance. This leads to:

$$Y = f\left(X_1^*, \dots, X_{i-1}^*, X_{i,0}, X_{i+1}^*, \dots, X_q^*\right) = Y\left(X_{i,0}, X_{j \neq i}^*\right) \tag{22}$$

Hence, the total variance reduction of such a model reads:

$$\Delta V_{j \neq i}^* = V(Y_0) - V\left(Y\left(X_{i,0}, X_{j \neq i}^*\right)\right) \tag{23}$$

Finally, modified first-order sensitivity indices S_i^* are obtained from the ratio of single variance reductions ΔV_i^* (Equation (20)) to the total one ΔV^* (acc. to Equation (18)). These indices capture the benefit of improving the knowledge about a single parameter X_i but neglecting any interactions with other reduced variances.

$$S_i^* = \frac{\Delta V_i^*}{\Delta V^*} = \frac{V(Y_0) - V(Y(X_{j \neq i,0}, X_i^*))}{V(Y_0) - V(Y^*)} \tag{24}$$

To evaluate the benefit of simultaneous measurements and belonging variance reductions of two or more parameters, higher-order modified sensitivity indices are conceivable, too.

$$S_{j \neq i}^* = \frac{\Delta V_{j \neq i}^*}{\Delta V^*} = \frac{V(Y_0) - V\left(Y\left(X_{i,0}, X_{j \neq i}^*\right)\right)}{V(Y_0) - V(Y^*)} \tag{25}$$

However, each index $S_{j \neq i}^*$ would require n additional model evaluations. In addition, relevant parameter combinations would have to be estimated in advance. Thus, such indices are omitted in the following evaluations.

3.2. Computational Implementation

A computational procedure to evaluate models is developed next. In general, it is based on the previously described computation of the original sensitivity indices in Section 2.2. An estimation of the modified sensitivity indices by correlation properties is no longer possible since the influence of reduced variances and the importance of a parameter would be mixed. A correlation coefficient analogue to the one in Equation (12) would still identify an important parameter even if its variance cannot be reduced. This is contrary to the basic idea of the modified sensitivity indices.

First, two sample matrices A^* and B are determined analogously to the procedure in Section 2.2. Since the indices are no longer determined with correlation coefficients approach, it does not matter, whether they are stochastically independent or not. However, the pre-defined correlation within the matrices (usually the parameters are supposed to be independent) still needs to be maintained. Now, A^* contains the realizations of reduced variance; B contains the realizations with the highest (initial) scatter. As before, both result vectors a^* and b are evaluated by employing the model.

$$a^* = Y(A^*) = Y(X_i^*) \tag{26}$$

$$b = Y(B) = Y(X_{i,0}) \tag{27}$$

Next, further q matrices C_i^* are generated. These matrices are assembled mainly from realizations of matrix B . Only column i comes from matrix A^* . For each c_i^* the model needs to be evaluated again n times.

$$c_i^* = Y(C_i^*) = Y(X_{j \neq i,0}, X_i^*) \tag{28}$$

Finally, the computation of the modified sensitivity index follows analogue to Equation (24).

$$S_i^* = 1 - \frac{V(c_i^*) - V(a^*)}{V(b) - V(a^*)} = \frac{V(b) - V(c_i^*)}{V(b) - V(a^*)} \tag{29}$$

4. Application Case: A Model for Fatigue Lifetime Prediction of Pre-Stressed Concrete Bridges

The variance-based sensitivity indices were modified to analyze a complex stochastic model, which was set up to predict the residual fatigue lifetime of aged pre-stressed concrete bridges. As a reference serves a 303 m long bridge in Germany [42]. Since the model includes, among other things, a finite element computation of the structural response and accumulation of damage over time, it is numerical and nondifferentiable. It involves interactions and uncertainties induced by the variance of the parameters. These different individual variances can be reduced, e.g., by on-site measurements, but, depending on the measurement methods and the individual aleatoric uncertainty, not to the same extent.

4.1. Reference Structure and Measurements

The reference structure for fatigue damage prediction is a 303 m long pre-stressed concrete bridge located in Düsseldorf, Germany (Figure 2). Since 1959, the box-girder-bridge has connected Düsseldorf’s city center to the German highway system. As it was a usual construction technique of that time, coupling joints connected consecutive construction parts and were located in each span at about one-fifth of the span length. The post-tensioned tendons had in general a parabolic profile, only few tendons ran straight along the upper and lower edges. Shortly after construction, first cracks were detected at the coupling joints. Because of the cracks and because it is a well-known weak point of aged bridges, fatigue of the tendons at the coupling joints was focused on during measurements and analyses.

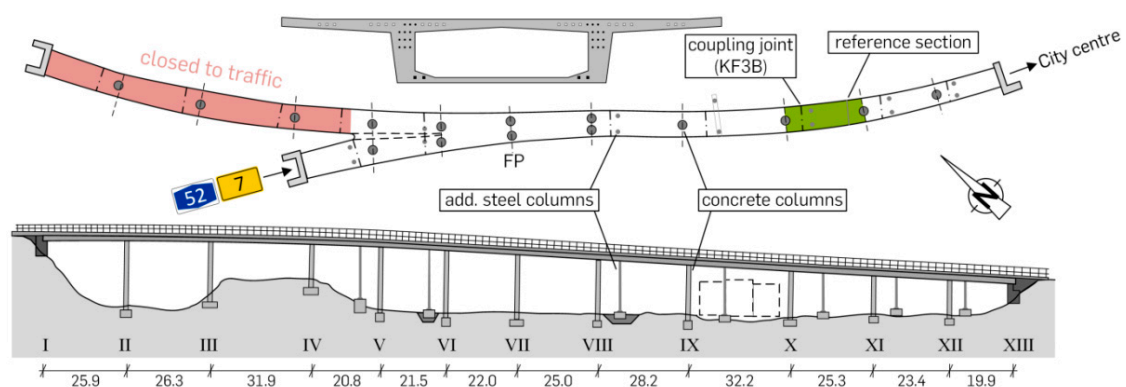


Figure 2. Reference structure Pariser Straße in Düsseldorf, Germany—side and top views along with a general cross-section.

On-site, different measurements were carried out on the structure. In view of its certain deconstruction and replacement, both destructive and nondestructive tests could be performed. To serve as a reference, many different measurements were carried out to cover a wide range of potential impacts increasing the accuracy. Here, the geometry was determined by length measurements on-site while the strength of concrete and of the pre-stressing steel were evaluated on concrete cores and steel samples in the lab. Additionally,

a strain monitoring of the pre-stressing steel and the temperature distribution (see Figure 3) was performed for several weeks.

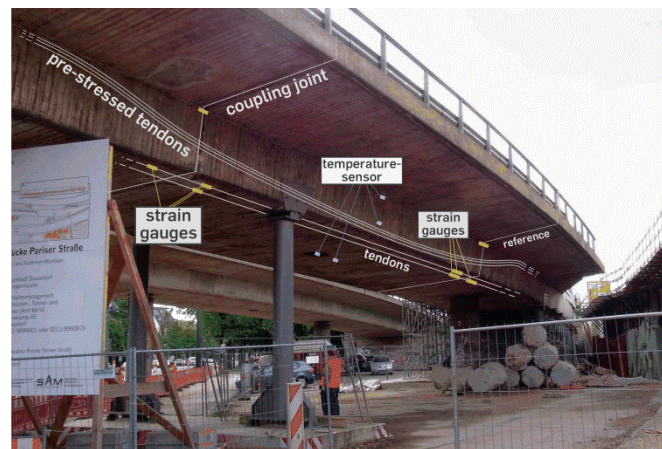


Figure 3. Strain and temperature monitoring of the reference structure.

4.2. Fatigue Lifetime Prediction Model for Pre-Stressed Concrete Bridges

An accurate prediction of the residual lifetime of pre-stressed concrete bridges, which are prone to fatigue, is hardly possible [43,44]. The special characteristic of high-cycle fatigue is sudden failure after many thousands or even millions of load cycles. For that, the fatigue damage progress is usually determined by extrapolating the frequency of calculated stress ranges from changing loads based on load models from the codes (e.g., [45]). Typical sources of uncertainty in the lifetime prediction for pre-stressed concrete road-bridges are:

- estimation and prognosis of loads (traffic loads and frequencies, temperature loads);
- calculation of stresses, including the nonlinearity after cracking (typically affected by the structural FE-model, cross-sectional and geometric parameters, material parameters, and stiffness);
- fatigue-related properties of the material resistance (represented by the $S-N$ curve).

The model considered here is nonlinear, time-dependent, and able to predict the fatigue lifetime T_{FL} of a pre-stressed concrete road-bridge, based on the accumulated fatigue damage D [46]. Fatigue failure occurs at damage $D = 1$ and is calculated by Miner’s rule [47,48]:

$$D = \sum_i \frac{n_i}{N_i} \leq 1 \tag{30}$$

Load frequencies n_i arise from traffic counts and prognosis and relative frequencies of individual vehicle types according to Eurocode 1–2 [45]. Load cycles until failure N_i are obtained from the $S-N$ curve (Figure 4) according to the stress ranges $\Delta\sigma_i$. Stress ranges are determined at different load levels i by combining a structural model and an iterative computation method of stresses. For convenience, the internal forces have been determined on a linear-elastic FE beam model (Figure 5) separated from the computation of stresses on cross-sectional level to reduce the computational costs. An advantage of this approach is that superposition of the internal forces can still be applied for all load cases and evaluations of the complex FE-model can be reduced. Then the stresses are computed, employing an iterative procedure by Krüger and Mertzsch [49] to get accurate stresses in cracked concrete conditions. To also cover non-cracked (linear elastic) conditions, the original approach was slightly modified and now permits the neutral strain fiber to lie outside the cross-section ($0 < \zeta \leq 2$, with $\zeta = x/d$ and x being the height of compression zone and d the effective height), too.

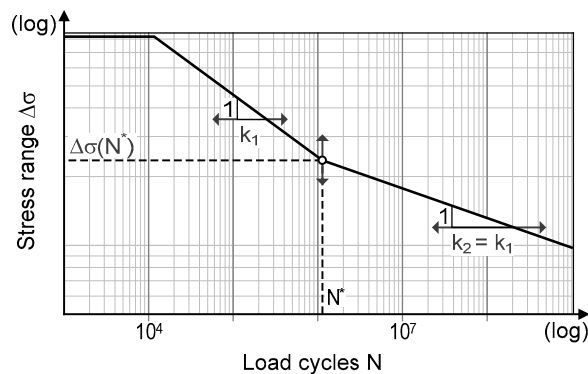


Figure 4. Typical S–N curve for high-strength steel and its variables indicated by arrows.

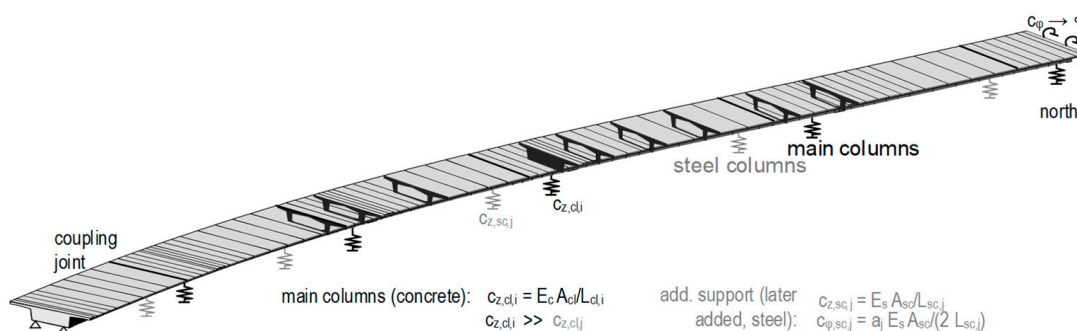


Figure 5. Finite-element model of the reference structure; beam elements (cross-sections for visualization) and boundary conditions by springs and supports.

That way, all stress ranges that are relevant for fatigue are treatable uniquely. In advance, the approach was checked to be sufficiently accurate and significantly reduces the computational effort for repeated simulation runs in comparison to a more detailed fatigue lifetime prognosis as presented elsewhere [50].

The evolution of fatigue damage is a nonlinear time-dependent process (exemplified in Figure 6), which is influenced, i.a., by creep and shrinkage and a global increase of traffic loads and frequencies (cf. Figure 6 and [43]). Hence, fatigue lifetime is usually determined by damage accumulation until failure occurs (Equation (30)). The simulations here aim to determine the total fatigue damage accumulated in 250 years $D(t = 250 a)$. In total, five time intervals ($\Delta t = 50 a$), are assumed to cover the prediction period. Obviously, this is a quite rough discretization of time—especially for the first years, where the gradients are usually steep—but it was necessary to reduce the computational costs.

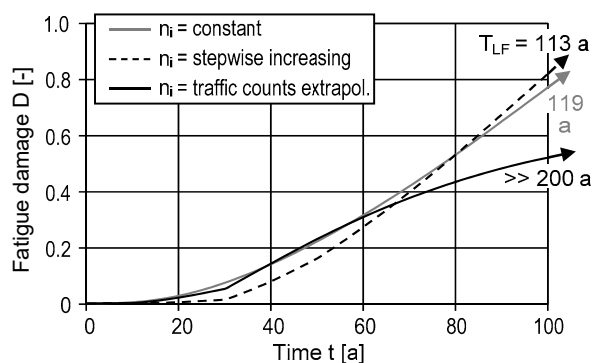


Figure 6. Damage evolution from a deterministic model with time-dependent stress ranges and three different approaches of the load frequency.

Creep, shrinkage and relaxation reduce the pre-strain in the tendons as a function of time. To cover creep and shrinkage, Bažant and Baweja’s model B3 [51] has been incorporated and simplified to a scaling function $a_{CS}(t)$ of the reduced pre-stress (details in [46]). Furthermore, hardening of concrete (compressive strength $f_c(t)$ and Young’s modulus E_c) is considered by a root function according to Eurocode 2 [52].

For traffic loads, the detailed fatigue load model FLM 4 from Eurocode 1–2 [45] was applied. It consists of five standardized truck types that are representative for heavyweight traffic in Europe. For convenience and to reduce the computational costs, the evaluations are restricted on truck type 3 of FLM 4 since it causes the highest stress ranges on the reference structure [50]. Mathematically, this simplification is conservative and delivers a lower bound of predicted lifetimes. Next, traffic- and temperature-induced stresses are superposed, while the latter ones have been computed from a histogram of discrete frequencies of linear vertical temperature gradients ΔT with time [53].

All the effects described before are considered in the model by 16 parameters:

- the width of the deck-slab b_f , which represents the variability of the entire geometry;
- the effective height d_{p1} of the pre-stressed cross-section concerning tendon layer no. 1;
- a scaling factor for pre-stress losses by creep and shrinkage a_{CS} ;
- five (relevant) linear temperature gradients ΔT_i ;
- a scaling factor w_3 for the traffic loads from FLM 4, truck no. 3;
- the cross-sectional area of a tendon A_{p1} ;
- Young’s moduli of concrete E_c and pre-stressing steel E_p ;
- two parameters to describe the $S-N$ curve: its knee point $\Delta\sigma(N^*)$ at 10^6 load cycles and the slope of the high-cycle fatigue range (k_2); for simplification k_1 is set equal to k_2 .

These parameters are all subjected to uncertainty (cf. Table 1). Following a probabilistic approach, their scatter can be captured by normal and log-normal probability density functions (PDF). Table 1 also provides individual means and variances.

Table 1. Stochastic variables with initial (original) distribution characteristics ($\mu_{i,0}$, $\sigma_{i,0}$) and reduced variances (σ_i^*), as well as Sobol’s sensitivity indices.

Variable i	Distribution	Orig. Distribution		Improvement		Sensitivity Indices		
		$\mu_{i,0}$	$CV_{i,0}$	CV_i^*	$V_i^*/V_{i,0}$	S_i	S_{π}	
Pre-strain	$\varepsilon_p^{(0)}$ [%o]	N	2.175	0.046	0.014	0.09	0.05	0.12
Young’s modulus of steel	E_p [N/mm ²]	N	205,000	0.030	0.024	0.63	~0	0.06
Scaling factor for creep and shrinkage	a_{CS} [-]	N	1	0.100	0.050	0.25	0.18	0.26
Young’s modulus of concrete	E_c [N/mm ²]	LN	33,000	0.091	0.045	0.25	0.02	0.04
$S-N$ curve:								
knee point	$\Delta\sigma(N^*)$ [N/mm ²]	LN	120	0.008	0.063	0.88	0.11	0.11
slope	k_2 [-]	LN	7	0.071	0.043	0.36	0.004	0.01
Width of the deck-slab	b_f [m]	N	4.95	0.101	0.001	<0.01	0.01	0.05
Area of a tendon	A_{p1} [cm ²]	N	26.55	0.016	0.007	0.21	0.01	0.04
Effective height for tendon layer 1	d_{p1} [m]	N	1.31	0.008	0.002	0.04	0.002	0.02
Gradient of load cycles per year	dn/dt	N	15,000	0.333	0.317	0.9	0.02	0.02
Scaling factor for FLM4-type 3	w_3 [-]	N	1	0.100	0.100	1	~0	0.05
Temperature gradients (scaled):								
$\Delta T(-4 K)$		N	1	0.008	0.141	0.5	~0	0.02
$\Delta T(-5 K)$		N	1	0.200	0.141	0.5	0.01	0.04
$\Delta T(-6 K)$		N	1	0.200	0.141	0.5	0.06	0.18
$\Delta T(-7 K)$		N	1	0.200	0.141	0.5	0.18	0.29
$\Delta T(-8 K)$		N	1	0.200	0.141	0.5	0.14	0.24

In addition to the original distribution parameters ($\mu_{i,0}$, $CV_{i,0}$), the reduced variances (as improved variation coefficient CV^* with aleatory uncertainty only) are summarized in Table 1. The ratios of improved to original variances $V^*/V_0 = \sigma^{*2}/\sigma_0^2$ are a measure to assess the improvement of a single parameter. For values close to zero the improvement is significant, for $V_i^*/V_{i,0} = 1$ there is no reduction of the variance (by measurements). The given values are assumptions based on measurement data from the reference structure and information from the literature.

Original variance-based sensitivity indices S_i and S_{T_i} according to Section 2.1 (Figure 7, left) and reduced variances (as improved standard deviations σ^* and as ratios of improved to original variances V^*/V_0) are given as well in Table 1. Before the sensitivity indices are determined, the result is logarithmically transformed ($y_i = \log(x_i)$) to be more robust. Consequently, the data appears Gaussian distributed.

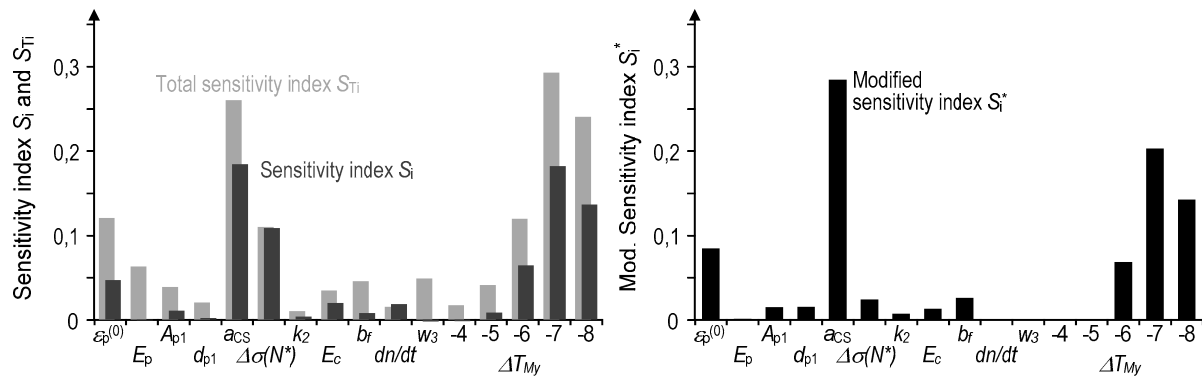


Figure 7. Original and total (left) versus modified sensitivity indices (right) for the reference bridge.

4.3. Stochastic Lifetime Prediction, Sensitivity Analysis and Evaluation of Modified Sensitivity Indices

The results of stochastic predictions of fatigue lifetime by Monte Carlo simulation are given in Table 2. They document a prognosis result when scatter of one single parameter is reduced by monitoring. More precisely, the table contains 16 sets of lognormal distribution characteristics $LN(\lambda, \zeta)$, means λ and standard deviations ζ , of accumulated damage D after 250 years. The shape of the distributions is assumed to be lognormal based on test statistics according to Kolmogorov–Smirnov (level of significance $\alpha = 0.05$). Each set is determined based on $n = 100$ simulations for each parameter ($n(2 + q) = 1800$).

Table 2. Improved distribution parameters, specific improvements of the target variable and modified sensitivity indices.

Variable i	Distribution Characteristics When i Is Improved				Relative Fractile Change		Mod. Sensitivity Index		
	λ	ζ	$D_{0,90}$	$D_{0,99}$	$D_{0,90}$	$D_{0,99}$	S_i^*		
Pre-strain	$\epsilon_p^{(0)}$	[‰]	−1.94	3.189	8.535	238.8	+11%	+16%	0.09
Young’s modulus of steel	E_p	[N/mm ²]	−1.93	3.254	9.350	280.2	+1%	+1%	0.001
Area of the tendon	A_{p1}	[cm ²]	−1.94	3.243	9.156	271.3	+3%	+4%	0.02
Effective depth of the tendon	d_{p1}	[m]	−1.93	3.243	9.283	275.0	+	+3%	0.02
Scaling factor creep and shrinkage	a_{CS}	[−]	−1.95	3.026	6.851	161.8	+31 %	+45%	0.29
S–N curve:									
knee point	$\Delta\sigma(N^*)$	[N/mm ²]	−1.92	3.236	9.291	273.2	+2%	+4%	0.03
slope	k_2	[−]	−1.93	3.249	9.324	278.0	+1%	+2%	0.01
Young’s modulus of concrete	E_c	[N/mm ²]	−1.97	3.245	8.893	263.9	+7%	+7%	0.01
Width of the deck-slab	b_f	[m]	−1.96	3.235	8.857	260.1	+7%	+9%	0.03
Gradient of load cycles in time	dn/dt		−1.93	3.257	9.406	282.7	+0%	+0%	−0
Scaling factor FLM4-type 3	w_3	[−]	−1.92	3.262	9.556	288.7	−%	−2%	−0
Temperature gradient:									
$\Delta T(−4 K)$			−1.96	3.284	9.469	292.8	−0%	−4%	−0
$\Delta T(−5 K)$			−1.98	3.260	9.004	271.4	+5%	+4%	−0
$\Delta T(−6 K)$			−2.08	3.201	7.519	213.2	+23%	+26%	0.07
$\Delta T(−7 K)$			−2.25	3.094	5.570	141.1	+46%	+53%	0.20
$\Delta T(−8 K)$			−2.19	3.143	6.268	167.1	+38%	+43%	0.14
“best” model a^* with V^*			−2.92	2.349	1.099	12.8	+100%	+100%	−
initial model b with V_0			−1.93	3.255	9.433	283.0	±0	±0	−

For comparison the characteristics for the initial model b (no improved variances) and the “best” model a^* (all variances improved) are listed in the lower rows, too. Additionally, two columns of the prognosis result’s fractiles $D_{0,90}$ and $D_{0,99}$ have been computed as characteristic values. For the fatigue damage, the upper bound of the distribution is of interest and focused. Additionally, in comparison to the improvement from the initial

model (b) to the best model (a*) the individual gains are quantified by relative specific improvements in the 6th and 7th column. The modified variance-based sensitivity indices are determined according to Equation (29) and are given in Table 2. They are also shown in Figure 7, right.

Next, original (S_i and S_{Ti}) and modified sensitivity indices (S_i^*) are opposed in Figure 7. For the presented fatigue lifetime model, at least six different variables show a significant impact (S_i and S_{Ti}) on the variance of the model. As a result of non-uniformly improved variances the results of the modified sensitivity indices (S_i^*) are individually shifted in comparison to the original sensitivity indices S_i and S_{Ti} in Table 2. Obviously, only relevant parameters characterized by a high sensitivity index S_{Ti} and a seriously reduced variance ($\sigma_{i,0} \gg \sigma_i^*$) lead to a significant variance reduction of the model. In contrast, a parameter without any variance reduction ($\sigma_{i,0} = \sigma_i^*$), like the scaling factor of traffic loads w_3 , does not change the model’s variance.

In total, three variables possess the highest original sensitivity indices: two temperature gradients $\Delta T(-7K)$, $\Delta T(-8K)$ and the scaling factor for creep and shrinkage a_{CS} . Since the variance of a_{CS} can be reduced at most (cf. Table 1) it also delivers the highest modified sensitivity index S_i^* (Figure 7, right)—as expected. The knee point of the $S-N$ curve $\Delta\sigma(N^*)$ is a moderately important variable ($S_i \approx S_{Ti} \approx 0.11$), but its variance can hardly be reduced by measurements. Thus, it exhibits a low modified sensitivity index $S_i^* = 0.03$.

The impact of individual improvements is illustrated by four probability density functions (PDF) in Figure 8. Referenced is the original model Y_0 with the highest variance—given by the computational result in b and marked by a dashed black line. This distribution function represents the initial prediction of the fatigue lifetime, having little knowledge about the parameters. Its total scatter comprises both, aleatory (random) and epistemic (lack of knowledge) parts. The “best” prediction model Y^* using the computational result in a* yields another pdf marked as a solid black line in Figure 8. It visualizes the response when all variances are reduced to the greatest extent. Then the scatter is caused by aleatory parts uniquely. Compared to Y_0 the variance of Y^* is significantly lower while the mean is shifted, too.

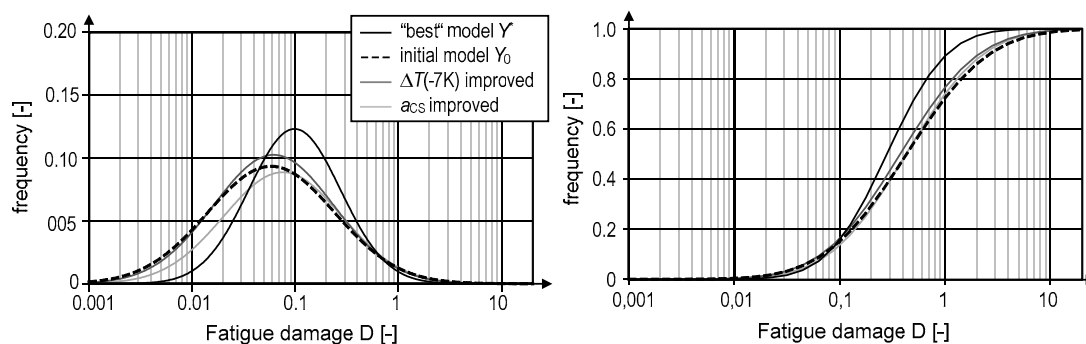


Figure 8. Probability and cumulative density functions of the original (Y_0) and the best model (Y^*) along with two cases when only one parameter’s scatter is reduced by monitoring.

Other cases when only one parameter’s variance is reduced by monitoring lie between these limit curves. The same holds true for the cumulative density functions (CDF) shown on the right in Figure 8. That way, the impact of individual measurements can be evaluated. Parameters that provide the closest shift to the “best” model yield the greatest benefit, if monitored. In this example, the scaling factor for creep and shrinkage a_{CS} and the linear temperature gradient $\Delta T(-7 K)$ are the most important. They shift both distributions (CDF and PDF) significantly towards the best model’s one. However, an irrelevant parameter would yield curves similar to the initial one.

4.4. Convergence

For reliable results, many thousand simulation runs are required as can be read from Figure 9 showing the convergence of the fatigue lifetime model. For the convergence plot the number of simulations n was increased incrementally from $n = 100$ to 10^4 . For each n , the modified sensitivity indices were determined ten times with different sampling sets to assess their variation around the mean x_m by means of the 5% and 95% fractiles ($x_m \pm 1.645 \cdot \sigma$, assuming a Gaussian distribution) as a measure of variance. The results of the modified sensitivity indices for some of the 16 parameters are drawn in Figure 9. The selection comprises three types of parameters:

- The scaling factor of the pre-stress loss a_{CS} in Figure 9 top left is a relevant parameter (S_{Ti} -value is high) and can be reduced significantly ($V_i^*/V_{i,0} \ll 1$). Therefore, its modified sensitivity index S_i^* is expected to be high.
- The knee point of the $S-N$ curve $\Delta\sigma(N^*)$ in Figure 9 top right is a relevant parameter (high S_{Ti} -value) without significant variance reduction ($V_i^*/V_{i,0} \approx 1$); thus, S_i^* is expected to be low.
- Third, the effective depth of the pre-stressing steel (d_{p1}) on the lower left of Figure 9 has a low (original) total sensitivity index S_{Ti} and even in case of a significant reduction of its variance, the modified sensitivity index can be expected to be low.

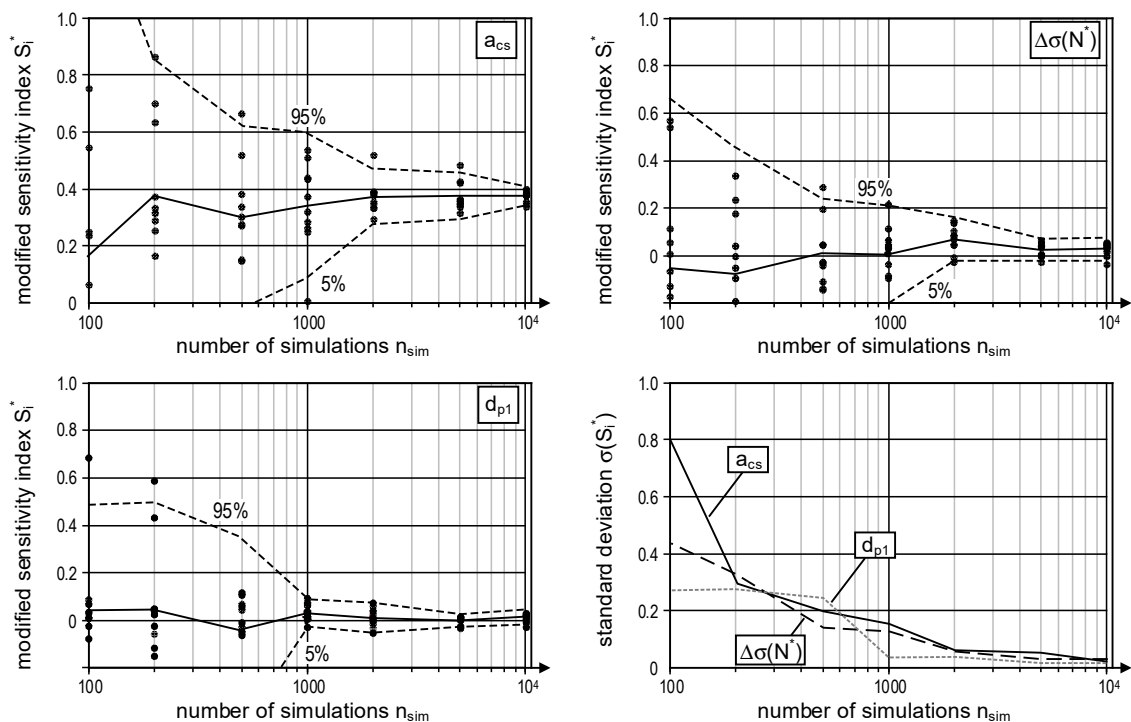


Figure 9. Convergence of the modified sensitivity index for three parameters of the lifetime prediction model.

All three clearly converge for 10^4 simulations. At least 5000 simulation runs are recommended in this case. For smaller sample sizes, all modified sensitivity indices possess large variance. For less than 1000 simulations, the results should not be used at all. Then, some results with too-small sample sizes take on values even outside the reasonable range $0 \leq S_i^* \leq 1$. As it could be expected, this is more likely for S_i^* -values close to zero. On the lower right, Figure 9 illustrates the convergence by means of the standard deviation. All three parameters converge similarly. Differences are seen purely caused by chance.

5. Conclusions

An extension to the established method of variance-based sensitivity indices originally proposed by Sobol' is developed. The modified sensitivity indices are suited to quantify

potential benefits of measurements and monitoring measures in advance. The enhanced indices are mathematically derived, and its numerical implementation based on stochastic simulation is exemplified on a model for fatigue lifetime prediction of a reference structure.

For the 50-year-old pre-stressed concrete bridge in Germany, the indices indicate that the measurement of residual pre-stress in the tendons after creep and shrinkage and the measurement of temperature loads are most meaningful. It can be found that the best parameters to be measured (high S_i^*) are those impairing a model's variance significantly (characterized by high-variance-based indices S_i and S_{Ti}) and simultaneously having a great potential for variance reduction by monitoring. In comparison to others, they possess the highest modified sensitivity indices.

To support experts' sound decisions on qualified measures to take the complex interaction of variance reduction and its influence on a model can be assessed in advance and quantified with reasonable effort by the newly proposed modified sensitivity indices S_i^* . In view of an ever-increasing stock of aged infrastructure buildings worldwide, the modified indices might help to save money and resources, avoiding unnecessary measurements in the future.

Author Contributions: Conceptualization, D.S., M.A.A. and P.M.; methodology, D.S.; software, D.S.; investigation, D.S.; data curation, D.S.; validation, D.S. and M.A.A.; writing—original draft preparation, D.S.; writing—review and editing, M.A.A. and P.M.; visualization, D.S.; supervision, M.A.A. and P.M.; project administration, M.A.A.; funding acquisition, M.A.A. and P.M. All authors have read and agreed to the published version of the manuscript.

Funding: This research was funded by the German Research Foundation (Deutsche Forschungsgemeinschaft DFG), grant number 221282822.

Institutional Review Board Statement: Not applicable.

Informed Consent Statement: Not applicable.

Data Availability Statement: The datasets generated during the study are available from the corresponding author on reasonable request.

Conflicts of Interest: The authors declare no conflict of interest.

References

- Ahrens, M.A.; Mark, P. Lebensdauersimulation von Betontragwerken. *Beton- und Stahlbetonbau*. **2011**, *106*, 220–230. [[CrossRef](#)]
- Sanio, D.; Ahrens, M.A. Identification of relevant but stochastic input parameters for fatigue assessment of pre-stressed concrete bridges by monitoring. In Proceedings of the 1st International Conference on Uncertainty Quantification in Computational Sciences and Engineering (UNCECOMP 2015), Crete Island, Greece, 25–27 May 2015; Papadrakakis, M., Papadopoulos, V., Stefanou, G., Eds.; pp. 947–960.
- Ambrozinski, L.; Packo, P.; Pieczonka, L.; Stepinski, T.; Uhl, T.; Staszewski, W.J. Identification of material properties—efficient modelling approach based on guided wave propagation and spatial multiple signal classification. *Struct. Control. Health Monit.* **2015**, *22*, 969–983. [[CrossRef](#)]
- Žnidarič, A.; Kreslin, M.; Lavrič, I.; Kalin, J. Simplified Approach to Modelling Traffic Loads on Bridges. *Procedia Soc. Behav. Sci.* **2012**, *48*, 2887–2896. [[CrossRef](#)]
- Löschmann, J.; Ahrens, A.; Dankmeyer, U.; Ziem, E.; Mark, P. Methoden zur Reduktion des Teilsicherheitsbeiwerts für Eigenlasten bei Bestandsbrücken. *Beton. Und. Stahlbetonbau*. **2017**, *112*, 506–516. [[CrossRef](#)]
- Ahrens, M.A. Precision-assessment of lifetime prognoses based on SN-approaches of RC-structures exposed to fatigue loads. In Life-Cycle and Sustainability of Civil Infrastructure Systems. In Proceedings of the 3rd International Symposium on Life-Cycle Civil Engineering (IALCCE), IALCCE 12, Vienna, Austria, 3–6 October 2012; Strauss, A., Frangopol, D., Berg-Meister, K., Eds.; CRC Press: Hoboken, NJ, USA, 2012; p. 109, ISBN 9780203103364.
- Gao, R.; Li, J.; Ang, A.H.-S. Stochastic analysis of fatigue of concrete bridges. *Struct. Infrastruct. Eng.* **2019**, *15*, 925–939. [[CrossRef](#)]
- Walpole, R.E.; Myers, R.H.; Myers, S.L.; Ye, K. *Probability & Statistics for Engineers & Scientists*, 9. Auflage; Prentice Hall: Boston, MS, USA, 2012; ISBN 0321629116.
- Strauss, A.; Hoffmann, S.; Wan-Wendner, R.; Bergmeister, K. Structural assessment and reliability analysis for existing engineering structures, applications for real structures. *Struct. Infrastruct. Eng.* **2009**, *5*, 277–286. [[CrossRef](#)]
- Saltelli, A.; Ratto, M.; Andres, T.; Campolongo, F.; Cariboni, J.; Gatelli, D.; Saisana, M.; Tarantola, S. *Global Sensitivity Analysis: The Primer*; John Wiley & Sons: Chichester, UK, 2008; ISBN 0470725176.

11. Iooss, B.; Lemaître, P. A review on global sensitivity analysis methods // A Review on Global Sensitivity Analysis Methods. In *Uncertainty Management in Simulation–Optimization of Complex Systems: Algorithms and Applications*, Dellino, G., Meloni, C., Eds.; Springer: Boston, MA, USA, 2015; pp. 101–122. ISBN 978-1-4899-7546-1.
12. Augusti, G.; Baratta, A.; Casciati, F. *Probabilistic Methods in Structural Engineering*; Chapman and Hall/CRC: Boca Raton, FL, USA, 2014; ISBN 9781482267457.
13. Saltelli, A.; Annoni, P.; Azzini, I.; Campolongo, F.; Ratto, M.; Tarantola, S. Variance based sensitivity analysis of model output. Design and estimator for the total sensitivity index. *Comput. Phys. Commun.* **2010**, *181*, 259–270. [[CrossRef](#)]
14. Wainwright, H.M.; Finsterle, S.; Jung, Y.; Zhou, Q.; Birkholzer, J.T. Making sense of global sensitivity analyses. *Comput. Geosci.* **2014**, *65*, 84–94. [[CrossRef](#)]
15. Sanio, D.; Obel, M.; Mark, P. Screening methods to reduce complex models of existing structures. In Proceedings of the 17th International Probabilistic Workshop (IPW), Edinburgh, UK, 11–13 September 2019; pp. 51–56.
16. Campolongo, F.; Cariboni, J.; Saltelli, A. An effective screening design for sensitivity analysis of large models. *Environ. Model. Softw.* **2007**, *22*, 1509–1518. [[CrossRef](#)]
17. Morris, M.D. Factorial Sampling Plans for Preliminary Computational Experiments. *Technometrics* **1991**, *33*, 161. [[CrossRef](#)]
18. Sobol, I.M. Global sensitivity indices for nonlinear mathematical models and their Monte Carlo estimates. *Math. Comput. Simul.* **2001**, *55*, 271–280. [[CrossRef](#)]
19. Campolongo, F.; Tarantola, S.; Saltelli, A. Tackling quantitatively large dimensionality problems. *Comput. Phys. Commun.* **1999**, *117*, 75–85. [[CrossRef](#)]
20. Bien, J.; Kuźawa, M.; Kamiński, T. Strategies and tools for the monitoring of concrete bridges. *Struct. Concr.* **2020**, *21*, 1227–1239. [[CrossRef](#)]
21. Brühwiler, E. Fatigue safety examination of riveted railway bridges using monitored data. In *Bridge Maintenance, Safety, Management and Life Extension, Proceedings of the 7th International Conference of Bridge Maintenance, Safety and Management. IABMAS 2014, Shanghai, China, 7–11 July 2014*; Chen, A., Frangopol, D.M., Eds.; CRC Press: Boca Raton, FL, USA, 2014; pp. 1169–1176. ISBN 9781138001039.
22. Frangopol, D.M.; Strauss, A.; Kim, S. Bridge Reliability Assessment Based on Monitoring. *J. Bridg. Eng.* **2008**, *13*, 258–270. [[CrossRef](#)]
23. Bayane, I.; Mankar, A.; Brühwiler, E.; Sørensen, J.D. Quantification of traffic and temperature effects on the fatigue safety of a reinforced-concrete bridge deck based on monitoring data. *Eng. Struct.* **2019**, *196*, 109357. [[CrossRef](#)]
24. Treacy, M.A.; Brühwiler, E. Action effects in post-tensioned concrete box-girder bridges obtained from high-frequency monitoring. *J. Civ. Struct. Health Monit.* **2014**, *5*, 11–28. [[CrossRef](#)]
25. Nair, A.; Cai, C.S. Acoustic emission monitoring of bridges: Review and case studies. *Eng. Struct.* **2010**, *32*, 1704–1714. [[CrossRef](#)]
26. Marx, S.; von der Haar, C.; Liebig, J.P.; Grünberg, I.J. Bestimmung der Verkehrseinwirkung auf Brückentragwerke aus Messungen an Fahrbahnübergangskonstruktionen. *Bautech* **2013**, *90*, 466–474. [[CrossRef](#)]
27. Uva, G.; Porco, F.; Fiore, A.; Mezzina, M. Proposal of a methodology for assessing the reliability of in situ concrete tests and improving the estimate of the compressive strength. *Constr. Build. Mater.* **2013**, *38*, 72–83. [[CrossRef](#)]
28. Malhotra, V.M. *In Situ/Nondestructive Testing of Concrete*; American Concrete Institute (ACI): Detroit, MI, USA, 1984.
29. Der Kiureghian, A.; Ditlevsen, O. Aleatory or epistemic? Does it matter? *Struct. Saf.* **2009**, *31*, 105–112. [[CrossRef](#)]
30. Zhou, L.; Yan, G.; Wang, L.; Ou, J. Review of Benchmark Studies and Guidelines for Structural Health Monitoring. *Adv. Struct. Eng.* **2013**, *16*, 1187–1206. [[CrossRef](#)]
31. ACI Committee 444. PRC-444.2-21: Structural Health Monitoring Technologies for Concrete Structures. Report; ACI Reports ACI PRC-444.2-21, Farmington Hills, Mich. 2021. Available online: <https://www.concrete.org/store/productdetail.aspx?ItemID=444221> (accessed on 18 August 2021).
32. Pozo, F.; Tibaduiza, D.; Vidal, Y. Sensors for Structural Health Monitoring and Condition Monitoring. *Sensors* **2021**, *21*, 1558. [[CrossRef](#)]
33. Tarantola, S.; Gatelli, D.; Mara, T. Random balance designs for the estimation of first order global sensitivity indices. *Reliab. Eng. Syst. Saf.* **2006**, *91*, 717–727. [[CrossRef](#)]
34. Hora, S.C.; Iman, R.L. Comparison of Maximus/Bounding and Bayes/Monte Carlo for Fault Tree Uncertainty Analysis. 1986. Available online: <https://www.osti.gov/biblio/5824798> (accessed on 22 October 2021).
35. Cukier, R.I.; Levine, H.B.; Shuler, K.E. Nonlinear sensitivity analysis of multiparameter model systems. *J. Comput. Phys.* **1978**, *26*, 1–42. [[CrossRef](#)]
36. Sobol, I. Theorems and examples on high dimensional model representation. *Reliab. Eng. Syst. Saf.* **2003**, *79*, 187–193. [[CrossRef](#)]
37. Archer, G.E.B.; Saltelli, A.; Sobol, I.M. Sensitivity measures, anova-like Techniques and the use of bootstrap. *J. Stat. Comput. Simul.* **1997**, *58*, 99–120. [[CrossRef](#)]
38. Ökten, G.; Liu, Y. Randomized quasi-Monte Carlo methods in global sensitivity analysis. *Reliab. Eng. Syst. Saf.* **2021**, *210*, 107520. [[CrossRef](#)]
39. Glen, G.; Isaacs, K. Estimating Sobol sensitivity indices using correlations. *Environ. Model. Softw.* **2012**, *37*, 157–166. [[CrossRef](#)]
40. Saltelli, A.; Tarantola, S.; Chan, K.P.-S. A Quantitative Model-Independent Method for Global Sensitivity Analysis of Model Output. *Technometrics* **1999**, *41*, 39–56. [[CrossRef](#)]

41. Piano, S.L.; Ferretti, F.; Puy, A.; Albrecht, D.; Saltelli, A. Variance-based sensitivity analysis: The quest for better estimators and designs between explorativity and economy. *Reliab. Eng. Syst. Saf.* **2021**, *206*, 107300. [[CrossRef](#)]
42. Sanio, D.; Ahrens, M.A.; Mark, P.; Rode, S. Untersuchung einer 50 Jahre alten Spannbetonbrücke zur Genauigkeitssteigerung von Lebensdauerprognosen. *Beton- und Stahlbetonbau.* **2014**, *109*, 128–137. [[CrossRef](#)]
43. Sanio, D.; Ahrens, M.; Mark, P. Detecting the limits of accuracy of lifetime predictions by structural monitoring. In Proceedings of the Bridge Maintenance, Safety, Management and Life Extension; Chen, A., Frangopol, D.M., Eds.; CRC Press: Boca Raton, FL, USA, 2014; pp. 416–423.
44. Sanio, D.; Ahrens, M.A.; Mark, P. Tackling uncertainty in structural lifetime evaluations. *Beton- und Stahlbetonbau.* **2018**, *113*, 48–54. [[CrossRef](#)]
45. EN 1991-2: Eurocode 1: Actions on Structures: Part 2: Traffic Loads on Bridges; CEN: Brussels, Belgium, 2010.
46. Sanio, D. Accuracy of Monitoring-Based Lifetime-Predictions for Prestressed Concrete Bridges Prone to Fatigue. Ph.D. Thesis, Ruhr-Universität Bochum, Bochum, Germany, 2017.
47. Palmgren, A. Die Lebensdauer von Kugellagern. *Z. Des Ver. Dtsch. Ing.* **1924**, *68*, 339–341.
48. Miner, M.A. Cumulative Damage in Fatigue. *J. Appl. Mech.* **1945**, *12*, A159–A164. [[CrossRef](#)]
49. Krüger, W.; Mertzsch, O. Zum Trag- und Verformungsverhalten bewehrter Betonquerschnitte im Grenzzustand der Gebrauchstauglichkeit; DAfStb-Heft No. 533; Beuth: Berlin, Germany, 2006.
50. Sanio, D.; Ahrens, M.A.; Mark, P. Lifetime predictions of pre-stressed concrete bridges—Evaluating parameters of relevance using Sobol’-indices. *Civ. Eng. Des.* **2021**. [[CrossRef](#)]
51. Bažant, Z.P.; Baweja, S. Creep and shrinkage prediction model for analysis and design of concrete structures—model B3. *Mater. Struct.* **1995**, *28*, 357–365. [[CrossRef](#)]
52. EN 1992-2: Eurocode 2: Design of Concrete Structures: Part 2: Concrete Bridges—Design and Detailing Rules; CEN: Brussels, Belgium, 2010.
53. Sanio, D.; Mark, P.; Ahrens, M.A. Temperaturfeldberechnung für Brücken. *Beton- und Stahlbetonbau.* **2017**, *112*, 85–95. [[CrossRef](#)]